



Original

Pathogenesis of murine astrovirus in experimentally infected mice

Hanako MORITA¹⁾, Masahiko YASUDA²⁾, Masafumi YAMAMOTO¹⁾, Yurina TOMIYAMA¹⁾, Ritsuki UCHIDA³⁾, Yuyo KA⁴⁾, Tomoyuki OGURA⁴⁾, Kenji KAWAI²⁾, Hiroshi SUEMIZU⁵⁾ and Nobuhito HAYASHIMOTO¹⁾

¹⁾ICLAS Monitoring Center, Central Institute for Experimental Animals, 3-25-12 Tonomachi, Kawasaki-ku, Kawasaki, Kanagawa 210-0821, Japan

²⁾Pathology Analysis Center, Central Institute for Experimental Animals, 3-25-12 Tonomachi, Kawasaki-ku, Kawasaki, Kanagawa 210-0821, Japan

³⁾JAC Inc., No. 44 Kouwa building, 1-2-7 Higashiyama, Meguro-ku, Tokyo 153-0043, Japan

⁴⁾Animal Resource Technology Center, Central Institute for Experimental Animals, 3-25-12 Tonomachi, Kawasaki-ku, Kawasaki, Kanagawa 210-0821, Japan

⁵⁾Laboratory Animal Research Department, Biomedical Research Laboratory, Central Institute for Experimental Animals, 3-25-12 Tonomachi, Kawasaki-ku, Kawasaki, Kanagawa 210-0821, Japan

Abstract: Astroviruses are often associated with gastrointestinal diseases in mammals and birds. Murine astrovirus (MuAstV) is frequently detected in laboratory mice. Previous studies on MuAstV in mice did not report any symptoms or lesions. However, little information is available regarding its pathogenicity in immunodeficient mice. Therefore, in this study, we experimentally infected germ-free NOD.Cg-Prkdc^{scid}Il2rg^{tm1Sug}/ShiJic (NOG) mice, which are severely immunodeficient, with MuAstV. Germ-free mice were used for experimental infection to eliminate the effects of intestinal bacteria. Mice in each group were then necropsied and subjected to PCR for MuAstV detection, MuAstV RNA quantification in each organ, and histopathological examination at 4 and 28 days post inoculation (DPI). Tissue samples from the small intestine were examined by transmission electron microscopy. No symptoms or abnormalities were detected in any mice during necropsy. The MuAstV concentration was highest in the lower small intestine, where it increased approximately 8-fold from 4 to 28 DPI. Transmission electron microscopy revealed circular virus particles of approximately 25 nm in diameter in the cytoplasm of the villous epithelial cells of the lower small intestine. Histopathological examination did not reveal any abnormalities, such as atrophy, in the intestinal villi. Our results suggest that MuAstV proliferates in the villous epithelial cells of the lower small intestine and has weak pathogenicity.

Key words: experimental infection, mouse, murine astrovirus

Introduction

Astroviruses are nonenveloped, positive-sense, single-stranded RNA viruses often associated with gastrointestinal diseases in mammals and poultry [1]. They were first discovered by electron microscopy in 1975 in fecal samples from a human child with diarrhea [2]. They were first described as small viruses (28–30 nm in diameter)

with an icosahedral morphology, giving them a characteristic starlike appearance, from which their name (from the Greek word *astron*, meaning star) was derived [3]. Astroviruses are taxonomically divided into two groups, i.e., mamastroviruses (MAstVs), which infect mammals, and avastroviruses (AAstVs), which infect birds [1]. They infect a wide range of wild and domestic animals, including cows, sheep, pigs, turkeys, cats, dogs, and rats,

(Received 7 November 2020 / Accepted 4 March 2021 / Published online in J-STAGE 6 April 2021)

Corresponding author: H. Morita. e-mail: morita-h@ciea.or.jp



This is an open-access article distributed under the terms of the Creative Commons Attribution Non-Commercial No Derivatives (by-nc-nd) License <<http://creativecommons.org/licenses/by-nc-nd/4.0/>>.

©2021 Japanese Association for Laboratory Animal Science

marine mammals, and birds, causing diarrhea, enteritis, or sometimes no clinical signs [4]. They may also be associated with extra-gastrointestinal infections, such as encephalitis and meningitis [5–8]. Astroviruses cause little inflammation and cellular damage, and diarrhea in turkeys has been shown to be caused by disruption of the cellular tight junction complex in the intestinal epithelium by the astrovirus capsid protein [9–11]. Murine astrovirus (MuAstV)-like particles were first discovered in the gut contents of nude mice by electron microscopy during an episode of collective diarrhea in a mouse colony [12]. The complete genomic sequence of MuAstV was elucidated in 2011 in a metagenomic study of wild *Mus musculus* feces [13]. However, MuAstV has not been successfully cultured. MuAstV has been reported to retain infectivity even in soiled bedding stored for 3 weeks [14], and infection with MuAstV has been reported to increase intestinal permeability [9]. In recent years, MuAstV has been reported in laboratory mice worldwide [15, 16], and comparison of the MuAstV RNA-dependent RNA polymerase (RdRp) sequences showed numerous mutations indicating ongoing viral divergence in different facilities [15]. A positive rate of 35.0% was confirmed in a survey conducted in a laboratory animal facility in Japan in 2016 [17], and analysis of the RdRp gene in MuAstV detected in Japanese laboratory animal mice showed high similarity to various strains, including BSRI1 and STL1, in a public database [17]. There have been no case reports of MuAstV in mice, and no symptoms or lesions were confirmed in previous reports [14, 18, 19]. Limited information is available regarding its pathogenicity in immunodeficient mice [14, 15]. In recent years, immunodeficient mice with varying immunological characteristics have been produced and used as experimental animals; however, the details of MuAstV pathogenicity in immunodeficient mice remain unknown. Therefore, in this study, we examined the pathogenicity of MuAstV by experimental infection in germ-free NOD.Cg-Prkdc^{scid}Il2rg^{tm1Sug}/ShiJic (NOG) mice, which are severely immunodeficient [20]. Furthermore, histopathological examinations of the intestinal tract of spontaneously infected mice were performed.

Materials and Methods

Experimental infection

Experimental animals and rearing environment: Twenty-four germ-free NOG mice were used for experimental infection. NOG mice are severely immunodeficient and easily accept heterologous cells due to a deficiency of T-, B-, NK, and interferon-producing killer dendritic

cells, macrophage and dendritic cell dysfunction, and loss of complement activity [20]. To eliminate the effects of intestinal bacteria, germ-free mice were used for experimental infection. Germ-free mice were obtained from breeding colonies at the Central Institute for Experimental Animals (CIEA). The infected (n=12) and control (n=12) mice were maintained in sterilized vinyl isolators. The mice were individually identified, and three mice were housed in each cage. All mice and materials, including the sterilized feed and water, were aseptically loaded and unloaded through a sterile lock. All mice were confirmed to be MuAstV negative by PCR of fecal samples before the experiment. A sterility test was conducted before and after the experiment to ensure that sterile conditions were maintained throughout the experimental period.

Inoculation samples: Cecal samples were collected from NOG mice subjected to testing for microbial monitoring at the CIEA ICLAS Monitoring Center between November 2017 and December 2018, and PCR was performed to test for MuAstV. Cecal contents from 18 MuAstV-positive mice were mixed together, homogenized, and centrifuged, and the supernatant was sterilized by filtration using a 0.2- μ m filter, stored at -80°C , and used as the inoculation sample for the experimental group. All cecal samples were collected from the same institution. According to a BLAST search for the RdRp gene, the MuAstV in all the positive samples showed a higher homology with BSRI1 (Accession No. KC609001) than with any other strain. A homogenate of cecal contents from 16 MuAstV-negative mice was prepared using the same methods and used as the inoculation sample for the control group. Blood agar medium was then smeared with 100 μ l of MuAstV-positive and MuAstV-negative inoculation samples and incubated at 37°C for 48 h to confirm the absence of bacterial growth. In addition, the microbiological test items listed in Table 1 were confirmed to be negative by PCR [21–29].

Study design for experimental infection: Twenty-four 4-week-old female mice were included in this study. They were divided into two experimental groups of 12 mice each. Mice in the infected group were inoculated with 100 μ l of the MuAstV-positive inoculation sample, whereas those in the control group were inoculated with 100 μ l of the MuAstV-negative inoculation sample. Six mice from each of the two groups were euthanized by excess inhalation of isoflurane at 4 and 28 days post inoculation (DPI). Blood samples for PCR and quantitative RT-PCR (RT-qPCR) analyses were collected from all mice by cardiac puncture. In addition, the forestomach, glandular stomach, duodenum, upper small intestine, middle small intestine, lower small intestine, ce-

Table 1. Results of PCR for microbiological test items of cecal homogenates

Microorganism tested	Inoculated sample of the infected group	Inoculated sample of the control group
Ectromelia virus	–	–
Lactate dehydrogenase-elevating virus	–	–
Lymphocytic choriomeningitis virus	–	–
Mouse adenovirus type 1	–	–
Mouse cytomegalovirus	–	–
Mouse encephalomyelitis virus	–	–
Mouse hepatitis virus	–	–
Mouse minute virus	–	–
Murine norovirus	–	–
Mouse parvovirus	–	–
Mouse rotavirus	–	–
Pneumonia virus of mice	–	–
Polyoma virus	–	–
Reovirus type 3	–	–
Sendai virus	–	–
<i>Clostridium piliforme</i>	–	–
<i>Filobacterium rodentium</i>	–	–
<i>Helicobacter bilis</i>	–	–
<i>Helicobacter hepaticus</i>	–	–
<i>Mycoplasma pulmonis</i>	–	–
<i>Pneumocystis</i> spp.	–	–
<i>Aspiculuris tetraptera</i>	–	–
<i>Syphacia obvelata</i>	–	–
<i>Entamoeba muris</i>	–	–

cum, colon, rectum, liver, spleen, and kidney were collected for PCR, RT-qPCR, and histopathological examination. A small intestine sample was also collected for electron microscopy.

Prior to PCR, the gastrointestinal tract was washed with sterile PBS to remove the contents. The prepared PCR and RT-qPCR samples were stored at -80°C until further analysis. Samples collected for histopathological examination were fixed in 10% neutral buffered formalin and stored at 25°C until examination. Tissue samples for transmission electron microscopy (TEM) were fixed in 0.1 M phosphate buffer with 2% paraformaldehyde and 2% glutaraldehyde.

PCR and RT-qPCR for MuAstV: All samples were screened for MuAstV by PCR. RNA extraction and PCR conditions were as previously reported [17], and MuAstV-BF (5' GAATTTGACTGGACACGCTTTGA 3') and MuAstV-BR (5' GGTTTAACCCACATGCCAAA 3') primers, which target the RdRp gene, were used [15, 17]. The RNA extracted from each organ was adjusted to a concentration of 50 ng/ μl , and MuAstV was then quantified in the sample by RT-qPCR. MuAstV-specific RT-qPCR was performed using Brilliant III Ultra-Fast SYBR Green RT-qPCR Master Mix (Agilent Technologies, Santa Clara, CA, USA) with MuAstV-BF and MuAstV-BR primers on a 7500 Fast Real-Time PCR System (Thermo Fisher Scientific K.K., Tokyo, Japan). The RT-qPCR program was designed in our facility, and the amplification conditions were as follows: 50°C for

10 min, 95°C for 3 min, and then 40 cycles of 95°C for 5 s, 58°C for 30 s (decreasing by 0.2°C per cycle), and 72°C for 30 s. To quantify the MuAstV in the tested samples, the copy number of the target gene was determined by software using a prepared standard, and a melting curve was generated after measurement. A negative control was included in each reaction. The generated data was analyzed using 7500 Software v2.3 (Thermo Fisher Scientific K.K.).

Histopathological analysis: The collected forestomach, glandular stomach, duodenum, upper small intestine, middle small intestine, lower small intestine, cecum, colon, rectum, liver, spleen, and kidney samples were subjected to histopathological examination. Tissue samples were fixed in 10% neutral buffered formalin, embedded in paraffin, and stained with hematoxylin and eosin (HE), according to the standard procedures. For the lower small intestine, the length and depth of at least 3 villi and crypts, respectively, were measured per slide using the NDP.view2 image viewing software (Hamamatsu Photonics K.K., Shizuoka, Japan). The mean villi length and crypt depth from each slide were used for statistical analysis using one-way analysis of variance (ANOVA). Differences with a P -value <0.05 were considered statistically significant.

TEM analysis: Tissue samples for TEM were fixed in 0.1 M phosphate buffer with 2% paraformaldehyde and 2% glutaraldehyde and then postfixed in 2% osmium tetroxide in 0.1 M phosphate buffer for 2 h in an ice bath.

The specimens were then dehydrated in graded ethanol and embedded in epoxy resin. An ultramicrotome was used to prepare ultrathin sections, which were stained with uranyl acetate for 15 min and a lead staining solution for 5 min before being subjected to TEM (Hitachi H-7600 at 100 kV).

Ethics statement: This study was conducted in strict accordance with the Regulations for Animal Experimentation of the CIEA, which are based on the Guidelines for Proper Conduct of Animal Experiments (Science Council of Japan, 2006). The experimental protocol was approved by the Institutional Animal Care and Use Committee for Animal Experimentation of the CIEA (permit no. 18035A).

Histopathological examination of spontaneously MuAstV-infected mice

To confirm the pathological condition of spontaneously MuAstV-infected mice with resident intestinal bacteria, their small intestine was subjected to histopathological examination (November–December 2019). In total, 101 mice from 29 facilities that were subjected to microbiological monitoring tests performed at the CIEA ICLAS Monitoring Center were surveyed. The cecum was collected for PCR and stored at -80°C until analysis. The lower small intestine samples for histopathological examination were fixed in 10% neutral buffered formalin and stored at 25°C until examination. The cecal samples were screened using PCR, and samples from PCR-positive mice were histopathologically examined. The PCR and histopathological analyses were performed as described in the previous sections.

Results

Experimental infection of MuAstV

Appearance and necropsy findings: The mice were asymptomatic at both 4 and 28 DPI, and no abnormalities were observed. The results of necropsies performed at 4 and 28 DPI revealed no abnormal findings in any mice.

PCR and RT-qPCR analyses of each organ: The MuAstV-positive inoculation sample ($100\ \mu\text{l}$) inoculated into the infected group contained 2.9×10^9 molecules of MuAstV RNA, as confirmed by RT-qPCR. PCR analyses performed at 4 DPI yielded positive results for samples from the liver, kidney, and entire intestinal tract except the rectum. In addition, 4 of the 6 blood samples tested positive (Table 2). PCR analyses performed at 28 DPI yielded positive test results for the samples from the forestomach, kidney, blood, and entire intestinal tract except the rectum (Table 2). All samples from the control group yielded negative PCR results. The amount of MuAstV per ng RNA in each organ was quantified by RT-qPCR. The MuAstV concentration was highest in the lower small intestine at 4 and 28 DPI. The MuAstV concentration in the lower small intestine exhibited an approximately 8-fold increase from 4 to 28 DPI (Fig. 1).

Histopathological examination of major organs: No abnormalities were noted in the histopathological examination of the forestomach, glandular stomach, duodenum, upper small intestine, middle small intestine, lower small intestine, cecum, colon, rectum, liver, spleen, and kidney (Fig. 2). The villi length, crypt depth, and villus/crypt ratio in the lower small intestine of the infected group were not significantly different from those of the control group at 4 and 28 DPI ($P > 0.05$; Figs. 2 and 3).

Table 2. Results of the PCR analysis of tissue samples from different organs performed at 4 and 28 days post inoculation (DPI)

Organ	4 DPI						28 DPI					
	No. 1	No. 2	No. 3	No. 4	No. 5	No. 6	No. 1	No. 2	No. 3	No. 4	No. 5	No. 6
Forestomach	+	+	–	+	+	+	+	+	+	+	+	+
Glandular stomach	+	+	–	–	+	–	+	+	–	+	+	+
Duodenum	+	+	+	+	+	+	+	+	+	+	+	+
Small intestine (upper)	+	+	+	+	+	+	+	+	+	+	+	+
Small intestine (middle)	+	+	+	+	+	+	+	+	+	+	+	+
Small intestine (lower)	+	+	+	+	+	+	+	+	+	+	+	+
Cecum	+	+	+	+	+	+	+	+	+	+	+	+
Colon	+	+	+	+	+	+	+	+	+	+	+	+
Rectum	–	–	–	–	–	+	+	–	+	+	+	+
Liver	+	+	+	+	+	+	+	+	–	+	+	+
Kidney	+	+	+	+	+	+	+	+	+	+	+	+
Spleen	–	–	–	+	–	–	+	+	+	+	+	–
Blood	+	+	+	+	–	–	+	+	+	+	+	+
Bone marrow	NT	NT	NT	NT	NT	NT	+	+	+	+	–	+
Brain	NT	NT	NT	NT	NT	NT	+	+	–	+	+	+

NT: not tested.

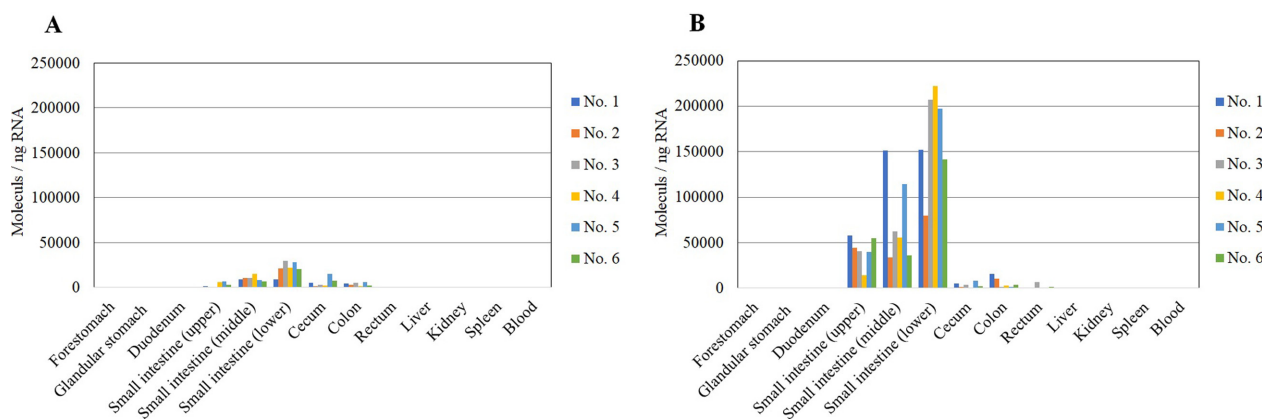


Fig. 1. Murine astrovirus (MuAstV) RNA concentration in each organ after MuAstV-positive cecal homogenate inoculation. A) 4 days post inoculation (DPI). B) 28 DPI.

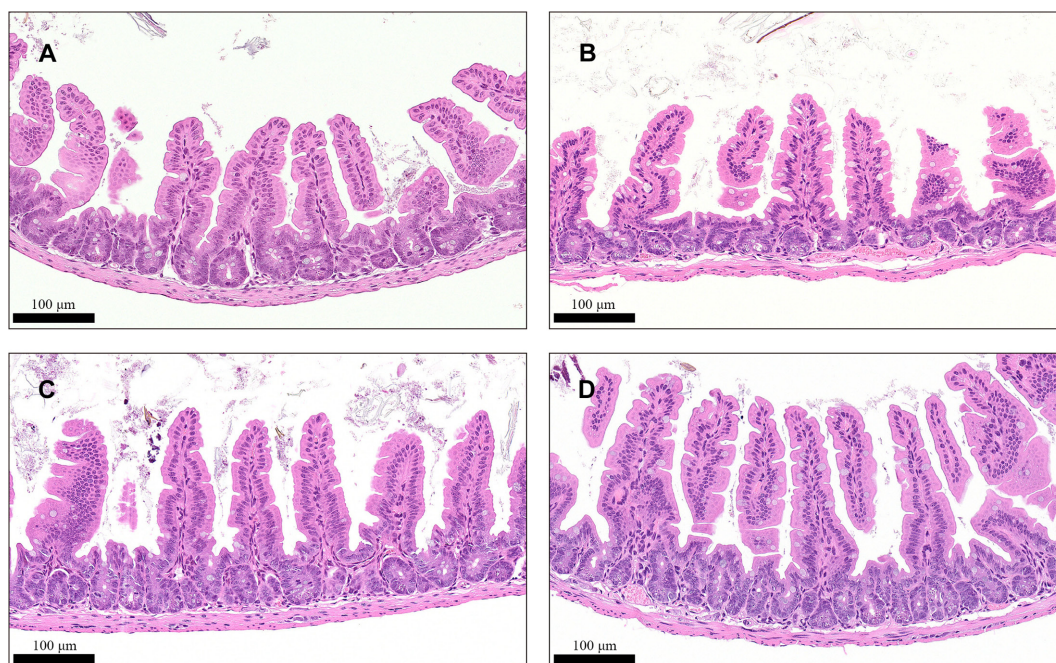


Fig. 2. Histopathological examination of the lower small intestine. (A) Murine astrovirus (MuAstV)-infected group at 4 days post inoculation (DPI). (B) Control group at 4 DPI. (C) MuAstV-infected group at 28 DPI. (D) Control group at 28 DPI.

TEM analysis of the lower small intestine: Tissue samples from the lower small intestine, where the MuAstV RNA concentration was highest, were examined by TEM. Circular virus particles of approximately 25 nm in diameter, forming electron-dense aggregates with a center-to-center distance of approximately 25 nm, were confirmed in the cytoplasm of the epithelial cells of the lower small intestine at both 4 and 28 DPI. Electron micrographs captured at 28 DPI are shown as representative examples (Fig. 4).

Histopathological examination of the small intestine of spontaneously MuAstV-infected mice

To investigate the effect of MuAstV on the spontane-

ous infection of mice with resident intestinal bacteria, 101 mice from 29 facilities monitored at the CIEA Monitoring Center were tested for MuAstV using PCR. Samples from 42 mice tested positive. Of these positive mice, 12, 6, 4, 4, 5, 8, and 3 belonged to the ICR, BALB/c, C57BL/6J, BALB/c-nu/+, BALB/c-nu/nu, SCID-beige, and NOG strains, respectively (Table 3). A histopathological examination of the small intestine was performed for these 42 MuAstV-positive mice, and no clinical signs or abnormal necropsy or histopathological findings were found for any of the mice.

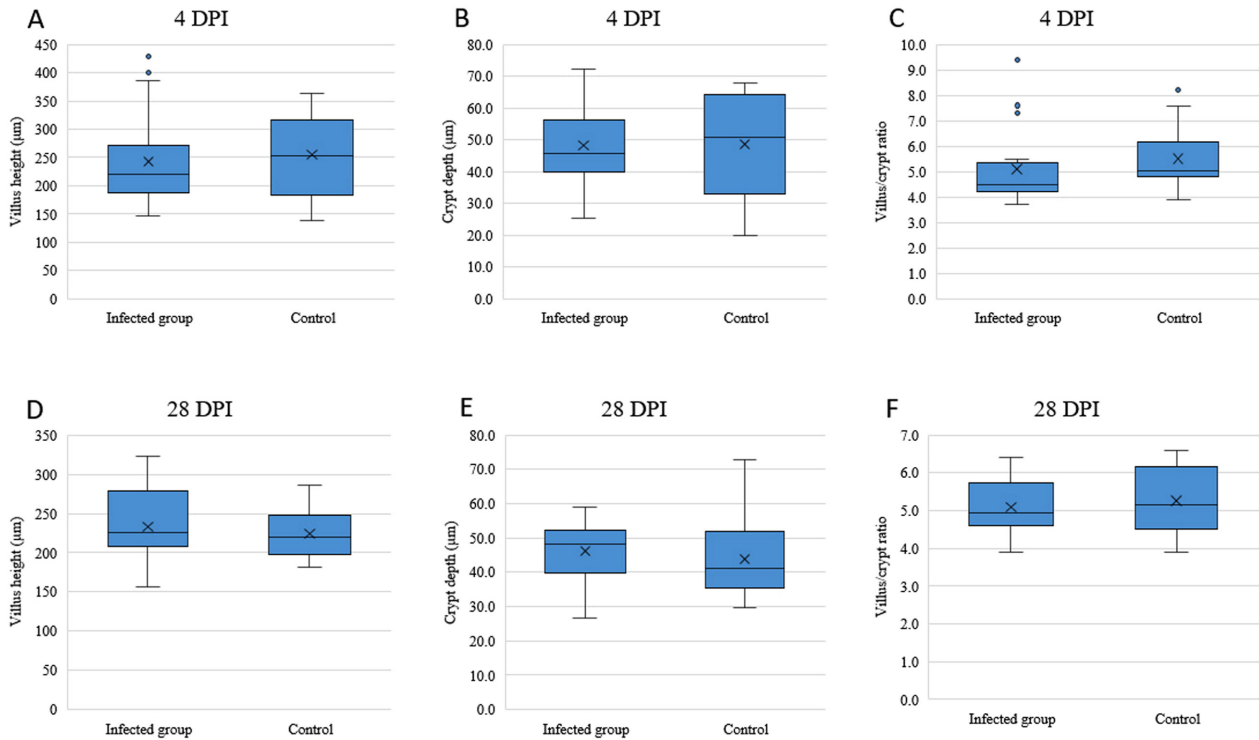


Fig. 3. Villus length, crypt depth, and villus/crypt ratio in the infected and control groups. (A) Villus length, (B) crypt depth, and (C) villus/crypt ratio at 4 days post inoculation (DPI). (D) Villus length, (E) crypt depth, and (F) villus/crypt ratio at 28 DPI. No significant differences were detected between the infected and control groups ($P>0.05$).

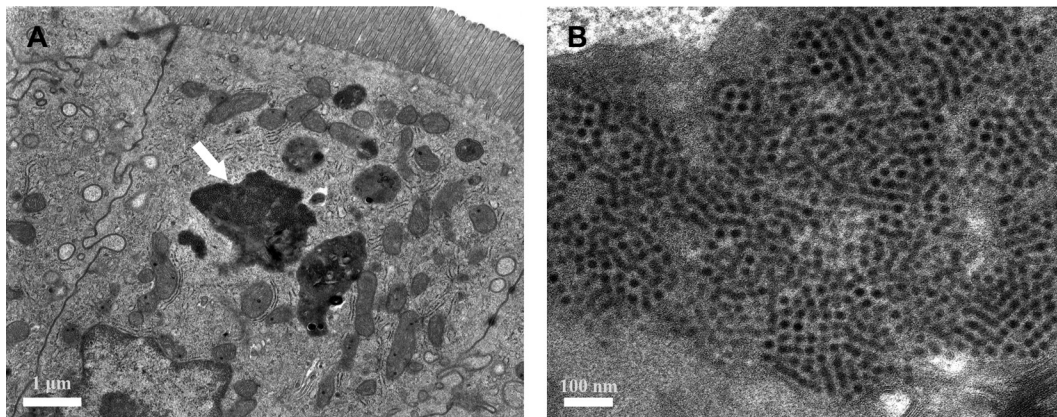


Fig. 4. Transmission electron microscopy of the lower small intestine. The ultrastructure of the lower small intestine of murine astrovirus (MuAstV)-infected mice was analyzed at 4 and 28 days post inoculation (DPI). (A and B) An electron micrograph of a sample analyzed 28 DPI is presented as a representative example. (A) Electron micrograph of the epithelial cells of a villus with viral aggregates in the cytoplasm (indicated by the white arrow) at 8,000 \times magnification. (B) Enlarged view of the region indicated by the white arrow at 50,000 \times magnification.

Discussion

RT-qPCR of tissue samples from each organ performed at 4 and 28 DPI revealed that the MuAstV concentration was highest in the lower small intestine, where it exhibited an approximately 8-fold increase from 4 to 28 DPI. In a previous report, the MuAstV concentration was found to be the highest in the duodenum of *Rag1*^{-/-} mice [18]; however, the effect of MuAstV present in the

intestinal contents was not described. In the present study, the intestinal samples were tested after the removal of intestinal contents with sterile PBS. TEM examination of the lower small intestine, where the MuAstV concentration was the highest, confirmed the presence of circular virus particles in the cytoplasm that were approximately 25 nm in diameter and forming aggregates with a center-to-center distance of approximately 25 nm; this suggests that in mice, MuAstV pro-

Table 3. Individual information of spontaneously murine astrovirus (MuAstV)-infected mice

Immunocompetent mice			Immunodeficient mice		
	Age (weeks)	Sex		Age (weeks)	Sex
ICR	17	Female	BALB/c-nu/nu	18	Female
ICR	17	Female	BALB/c-nu/nu	11	Unknown
ICR	12	Female	BALB/c-nu/nu	11	Unknown
ICR	17	Female	BALB/c-nu/nu	30	Female
ICR	17	Female	BALB/c-nu/nu	16	Female
ICR	17	Female	SCID-beige	18	Female
ICR	17	Female	SCID-beige	18	Female
ICR	8	Female	SCID-beige	18	Female
ICR	13	Female	SCID-beige	18	Female
ICR	13	Female	SCID-beige	18	Female
ICR	13	Female	SCID-beige	18	Female
ICR	16	Female	SCID-beige	18	Female
BALB/c	18	Male	SCID-beige	18	Female
BALB/c	18	Male	NOG	24	Male
BALB/c	18	Male	NOG	24	Male
BALB/c	18	Male	NOG	24	Male
BALB/c	18	Male			
BALB/c	18	Male			
C57BL/6J	23	Male			
C57BL/6J	8	Female			
C57BL/6J	24	Female			
C57BL/6J	12	Female			
BALB/c-nu/+	7	Female			
BALB/c-nu/+	24	Male			
BALB/c-nu/+	24	Male			
BALB/c-nu/+	30	Female			

liferates in the villous epithelial cells of the lower small intestine. Astroviruses are described as particles approximately 30 nm in diameter that are characterized by a starlike appearance [3]. However, in the present study, the particles often did not appear starlike; this observation is consistent with TEM observations of astroviruses in other animals [2, 30–32]. Although further confirmation by immunostaining is required, these results are consistent with those of previous reports on astrovirus infection in the intestinal villous epithelium of humans, pigs, lambs, and turkeys [30, 31, 33–35].

Following experimental infection in the present study, no clinical signs or abnormalities were observed during necropsy or histopathological examination of samples at 4 and 28 DPI. A previous study did not report any lesions in MuAstV-positive mice [14, 15, 19], which was also confirmed in the present study for more severely immunodeficient animals. Rotavirus, which infects the intestine, induces diarrhea by destroying the villous epithelial cells, ultimately causing cell death and villous atrophy [36, 37]. However, astroviruses have been reported to not cause cell death or visible histopathological changes [10, 19, 38], which is consistent with our results.

Enterovirus pathogenicity may be promoted or suppressed upon interaction with enterobacteria [39–41]. Therefore, germ-free mice were used for the infection

experiment to eliminate the effects of intestinal bacteria. In addition, 42 spontaneously MuAstV-infected mice with intestinal bacteria (both immunocompetent and immunodeficient) were selected for histopathological examination of the intestinal tract, and no abnormal necropsy findings, histopathological abnormalities, or clinical symptoms were observed in any of them; thus, there were no signs of promotion or suppression of MuAstV pathogenicity due to the presence or absence of intestinal bacteria.

Various mutations of MuAstVs have been reported based on comparison of the RdRp gene, and it is not possible to investigate the pathogenicity of all MuAstV strains. Therefore, in this study, BSRI1 (Accession No. KC609001), which is the most frequently detected MuAstV strain in Japan, and samples with the highest similarity were collected and used for experimental infection. The results of this study suggest that MuAstV proliferates in the villous epithelial cells of the lower small intestine of mice; however, it does not cause lesions, even in severely immunodeficient animals, such as NOG mice, and its pathogenicity is considered extremely weak. The CIEA ICLAS Monitoring Center, which conducts microbial monitoring tests for quality control of laboratory animals, classifies microorganisms into five categories (A to E) based on their pathogenicity in mice and rats [21], as follows: Category A, zoo-

notic and human pathogens carried by mice or rats; Category B, indigenous mouse or rat pathogens that can cause symptomatic disease and occasional death; Category C, microbes that usually cause asymptomatic infections accompanied by alterations in physiological functions; Category D, microbes that can cause opportunistic infections; Category E, microbes that are usually nonpathogenic but indicate the hygiene status of the rearing environment. Because viruses proliferate inside the cell, they are classified as Category C or higher; as a less pathogenic virus, MuAstV is considered to be in Category C. MuAstV retains infectivity for a long period of time and is orally transmitted. It has been reported that when sentinel mice were exposed to soiled bedding that had been stored for 1, 2, or 3 weeks before exposure, the feces of most sentinels became MuAstV positive [14]. In order to prevent MuAstV infection, as with other microorganisms, it may be necessary to use sterilized equipment, feed, and water for mice and to assign exclusive caretakers for areas that are confirmed to be MuAstV positive.

According to Compton *et al.*, MuAstV infection is not a confounding variable and does not affect the dextran sulfate-induced colitis model in NLRP3-deficient mice [42]; however, innate immunity is involved in the suppression of MuAstV proliferation [18]. MuAstV increases intestinal permeability; both C57BL/6 and IFN α R mice infected with MuAstV for 3 days had greater intestinal permeability than uninfected control mice, with IFN α R mice having a greater increase in permeability [9]. Turkey astrovirus causes diarrhea and sodium malabsorption [43], and the HAstV-1 capsid protein of the human astrovirus has been shown to disrupt the tight junction complex, thereby increasing barrier permeability [11]. When diarrhea occurred in a colony of nude mice in 1985, astrovirus-like virus particles were observed in the intestinal contents, but the diarrhea episode started during a heat wave in the summer when the temperature of the animal room was 22 to 32°C and the relative humidity varied between 25% and 70%. It has been suggested that the nude mice were previously symptomless carriers of MuAstV and that the pathogenicity of the virus was enhanced by the breakdown of climate control or by heavy experimental stress [12].

The results of this study reveal that the pathogenicity of MuAstV is extremely weak in mice, so it is not necessary to perform regular microbiological monitoring tests; however, it is considered that experiments related to immunity or intestinal permeability should check for MuAstV. Further studies are required to assess the effects of MuAstV infection on experiments in mice.

References

1. Johnson C, Hargest V, Cortez V, Meliopoulos VA, Schultz-Cherry S. Astrovirus Pathogenesis. *Viruses*. 2017; 9: 22. [[Medline](#)] [[CrossRef](#)]
2. Bosch A, Pintó RM, Guix S. Human astroviruses. *Clin Microbiol Rev*. 2014; 27: 1048–1074. [[Medline](#)] [[CrossRef](#)]
3. Donato C, Vijaykrishna D. The broad host range and genetic diversity of mammalian and avian astroviruses. *Viruses*. 2017; 9: 102. [[Medline](#)] [[CrossRef](#)]
4. De Benedictis P, Schultz-Cherry S, Burnham A, Cattoli G. Astrovirus infections in humans and animals - molecular biology, genetic diversity, and interspecies transmissions. *Infect Genet Evol*. 2011; 11: 1529–1544. [[Medline](#)] [[CrossRef](#)]
5. Quan PL, Wagner TA, Briese T, Torgerson TR, Hornig M, Tashmukhamedova A, et al. Astrovirus encephalitis in boy with X-linked agammaglobulinemia. *Emerg Infect Dis*. 2010; 16: 918–925. [[Medline](#)] [[CrossRef](#)]
6. Blomström AL, Widén F, Hammer AS, Belák S, Berg M. Detection of a novel astrovirus in brain tissue of mink suffering from shaking mink syndrome by use of viral metagenomics. *J Clin Microbiol*. 2010; 48: 4392–4396. [[Medline](#)] [[CrossRef](#)]
7. Li L, Diab S, McGraw S, Barr B, Traslavina R, Higgins R, et al. Divergent astrovirus associated with neurologic disease in cattle. *Emerg Infect Dis*. 2013; 19: 1385–1392. [[Medline](#)] [[CrossRef](#)]
8. Arruda B, Arruda P, Hensch M, Chen Q, Zheng Y, Yang C, et al. Porcine astrovirus type 3 in central nervous system of swine with polioencephalomyelitis. *Emerg Infect Dis*. 2017; 23: 2097–2100. [[Medline](#)] [[CrossRef](#)]
9. Marvin SA, Huerta CT, Sharp B, Freiden P, Cline TD, Schultz-Cherry S. Type I interferon response limits astrovirus replication and protects against increased barrier permeability in vitro and in vivo. *J Virol*. 2015; 90: 1988–1996. [[Medline](#)] [[CrossRef](#)]
10. Meliopoulos VA, Marvin SA, Freiden P, Moser LA, Nighot P, Ali R, et al. Oral administration of astrovirus capsid protein is sufficient to induce acute diarrhea in vivo. *MBio*. 2016; 7: e01494-16. [[Medline](#)] [[CrossRef](#)]
11. Moser LA, Carter M, Schultz-Cherry S. Astrovirus increases epithelial barrier permeability independently of viral replication. *J Virol*. 2007; 81: 11937–11945. [[Medline](#)] [[CrossRef](#)]
12. Kjeldsberg E, Hem A. Detection of astroviruses in gut contents of nude and normal mice. Brief report. *Arch Virol*. 1985; 84: 135–140. [[Medline](#)] [[CrossRef](#)]
13. Phan TG, Kapusinszky B, Wang C, Rose RK, Lipton HL, Delwart EL. The fecal viral flora of wild rodents. *PLoS Pathog*. 2011; 7: e1002218. [[Medline](#)] [[CrossRef](#)]
14. Compton SR, Booth CJ, Macy JD. Murine astrovirus infection and transmission in neonatal CD1 mice. *J Am Assoc Lab Anim Sci*. 2017; 56: 402–411. [[Medline](#)]
15. Ng TF, Kondov NO, Hayashimoto N, Uchida R, Cha Y, Beyer AI, et al. Identification of an astrovirus commonly infecting laboratory mice in the US and Japan. *PLoS One*. 2013; 8: e66937. [[Medline](#)] [[CrossRef](#)]
16. Schmidt K, Butt J, Mauter P, Vogel K, Erles-Kemna A, Pawlita M, et al. Development of a multiplex serological assay reveals a worldwide distribution of murine astrovirus infections in laboratory mice. *PLoS One*. 2017; 12: e0187174. [[Medline](#)] [[CrossRef](#)]
17. Morita H, Yasuda M, Yamamoto M, Uchida R, Tanaka M, Ishida T, et al. Prevalence of murine astrovirus in laboratory animal facilities in Japan. *J Vet Med Sci*. 2020; 82: 881–885. [[Medline](#)] [[CrossRef](#)]
18. Yokoyama CC, Loh J, Zhao G, Stappenbeck TS, Wang D, Huang HV, et al. Adaptive immunity restricts replication of novel murine astroviruses. *J Virol*. 2012; 86: 12262–12270. [[Medline](#)] [[CrossRef](#)]
19. Cortez V, Sharp B, Yao J, Livingston B, Vogel P, Schultz-

- Cherry S. Characterizing a murine model for astrovirus using viral isolates from persistently infected immunocompromised mice. *J Virol.* 2019; 93: e00223-19. [Medline] [CrossRef]
20. Ito M, Hiramatsu H, Kobayashi K, Suzue K, Kawahata M, Hioki K, et al. NOD/SCID/gamma(c)(null) mouse: an excellent recipient mouse model for engraftment of human cells. *Blood.* 2002; 100: 3175–3182. [Medline] [CrossRef]
 21. Hayashimoto N, Morita H, Ishida T, Yasuda M, Kameda S, Uchida R, et al. Current microbiological status of laboratory mice and rats in experimental facilities in Japan. *Exp Anim.* 2013; 62: 41–48. [Medline] [CrossRef]
 22. Ikegami T, Shiota K, Une Y, Nomura Y, Wada Y, Goto K, et al. Naturally occurring Tyzzer's disease in a calf. *Vet Pathol.* 1999; 36: 253–255. [Medline] [CrossRef]
 23. Harasawa R, Koshimizu K, Uemori T, Takeda O, Asada K, Kato I. The polymerase chain reaction for *Mycoplasma pulmonis*. *Microbiol Immunol.* 1990; 34: 393–395. [Medline] [CrossRef]
 24. Goto K, Nozu R, Takakura A, Matsushita S, Itoh T. Detection of cilia-associated respiratory bacillus in experimentally and naturally infected mice and rats by the polymerase chain reaction. *Exp Anim.* 1995; 44: 333–336. [Medline] [CrossRef]
 25. Tang-Feldman YJ, Wojtowicz A, Lochhead GR, Hale MA, Li Y, Pomeroy C. Use of quantitative real-time PCR (qRT-PCR) to measure cytokine transcription and viral load in murine cytomegalovirus infection. *J Virol Methods.* 2006; 131: 122–129. [Medline] [CrossRef]
 26. Goto K, Hayashimoto N, Ishida T, Takakura A, Kagiya N. First trial in the developmental phase of the “performance evaluation program” based on the ICLAS animal quality network program: self-assessment of microbiological monitoring methods using test samples supplied by ICLAS. *Exp Anim.* 2009; 58: 47–52. [Medline] [CrossRef]
 27. Hayashimoto N, Morita H, Ishida T, Uchida R, Tanaka M, Ozawa M, et al. Microbiological survey of mice (*Mus musculus*) purchased from commercial pet shops in Kanagawa and Tokyo, Japan. *Exp Anim.* 2015; 64: 155–160. [Medline] [CrossRef]
 28. Parel JD, Galula JU, Ooi HK. Characterization of rDNA sequences from *Syphacia obvelata*, *Syphacia muris*, and *Aspiculuris tetraptera* and development of a PCR-based method for identification. *Vet Parasitol.* 2008; 153: 379–383. [Medline] [CrossRef]
 29. Bootz F, Sieber I, Popovic D, Tischhauser M, Homberger FR. Comparison of the sensitivity of *in vivo* antibody production tests with *in vitro* PCR-based methods to detect infectious contamination of biological materials. *Lab Anim.* 2003; 37: 341–351. [Medline] [CrossRef]
 30. Sebire NJ, Malone M, Shah N, Anderson G, Gaspar HB, Cubitt WD. Pathology of astrovirus associated diarrhoea in a paediatric bone marrow transplant recipient. *J Clin Pathol.* 2004; 57: 1001–1003. [Medline] [CrossRef]
 31. Gray EW, Angus KW, Snodgrass DR. Ultrastructure of the small intestine in astrovirus-infected lambs. *J Gen Virol.* 1980; 49: 71–82. [Medline] [CrossRef]
 32. Woode GN, Pohlenz JF, Gourley NE, Fagerland JA. Astrovirus and Breda virus infections of dome cell epithelium of bovine ileum. *J Clin Microbiol.* 1984; 19: 623–630. [Medline] [CrossRef]
 33. Fang Q, Wang C, Liu H, Wu Q, Liang S, Cen M, et al. Pathogenic characteristics of a porcine astrovirus strain isolated in China. *Viruses.* 2019; 11: 1156. [Medline] [CrossRef]
 34. Snodgrass DR, Angus KW, Gray EW, Menzies JD, Paul G. Pathogenesis of diarrhoea caused by astrovirus infections in lambs. *Arch Virol.* 1979; 60: 217–226. [Medline] [CrossRef]
 35. Behling-Kelly E, Schultz-Cherry S, Koci M, Kelley L, Larsen D, Brown C. Localization of astrovirus in experimentally infected turkeys as determined by *in situ* hybridization. *Vet Pathol.* 2002; 39: 595–598. [Medline] [CrossRef]
 36. Crawford SE, Ramani S, Tate JE, Parashar UD, Svensson L, Hagbom M, et al. Rotavirus infection. *Nat Rev Dis Primers.* 2017; 3: 17083. [Medline] [CrossRef]
 37. Du J, Lan Z, Liu Y, Liu Y, Li Y, Li X, et al. Detailed analysis of BALB/c mice challenged with wild type rotavirus EDIM provide an alternative for infection model of rotavirus. *Virus Res.* 2017; 228: 134–140. [Medline] [CrossRef]
 38. Koci MD, Moser LA, Kelley LA, Larsen D, Brown CC, Schultz-Cherry S. Astrovirus induces diarrhea in the absence of inflammation and cell death. *J Virol.* 2003; 77: 11798–11808. [Medline] [CrossRef]
 39. Jones MK, Watanabe M, Zhu S, Graves CL, Keyes LR, Grau KR, et al. Enteric bacteria promote human and mouse norovirus infection of B cells. *Science.* 2014; 346: 755–759. [Medline] [CrossRef]
 40. Karst SM. The influence of commensal bacteria on infection with enteric viruses. *Nat Rev Microbiol.* 2016; 14: 197–204. [Medline] [CrossRef]
 41. Zhang B, Chassaing B, Shi Z, Uchiyama R, Zhang Z, Denning TL, et al. Viral infection. Prevention and cure of rotavirus infection via TLR5/NLRC4-mediated production of IL-22 and IL-18. *Science.* 2014; 346: 861–865. [Medline] [CrossRef]
 42. Compton SR, Booth CJ, Macy JD. Lack of effect of murine astrovirus infection on dextran sulfate-induced colitis in NLRP3-deficient mice. *Comp Med.* 2017; 67: 400–406. [Medline]
 43. Nighot PK, Moeser A, Ali RA, Blikslager AT, Koci MD. Astrovirus infection induces sodium malabsorption and redistributes sodium hydrogen exchanger expression. *Virology.* 2010; 401: 146–154. [Medline] [CrossRef]